Coalescence of viscous liquid drops

W. Yao, H. J. Maris, P. Pennington, and G. M. Seidel
Department of Physics, Brown University, Providence, Rhode Island 02912, USA
(Received 30 September 2004; published 13 January 2005)

We report on studies of the early stage of coalescence of two liquid drops. The drops were high viscosity silicon oil immersed in a water-alcohol mixture of the same density in order to eliminate the effects of gravity. The viscosity was sufficiently large that measurements could be made under the conditions of Stokes flow. Measurements were made of the radius of the neck between the drops as a function of the time from the onset of coalescence, and the results compared with theoretical predictions.

DOI: 10.1103/PhysRevE.71.016309 PACS number(s): 47.55.Dz, 47.20.Dr, 47.80.+v

I. INTRODUCTION

When two liquid drops come into contact, they may either bounce away from each other (noncoalescence) or merge into a single drop (coalescence). There are two aspects of this phenomena that are of interest: first, under what conditions the coalescence can start, and second, if coalescence does take place, how the shape of the two drops evolves with time. Rayleigh [1] and Reynolds [2] studied these phenomena. The study of coalescence is of importance in understanding processes such as raindrop formation, the separation of emulsions, and the sintering process. In this paper, we focus on the way in which the shape of liquid drops evolves during coalescence, and report on measurements of how the radius r_n of the neck between the drops varies as a function of time. We report on a series of measurements done with very viscous liquids such that the flow is in the Stokes regime, as discussed below. We restrict attention to the consideration of two drops with the same radius R_0 approaching each other with a very small relative velocity.

The parameters involved in the coalescence process are R_0, the viscosity η, the density ρ, and surface tension γ. From these parameters, we can construct the dimensionless Suratman number

$$\mathrm{Su} = \frac{\rho\gamma R_0}{\eta^2}, \tag{1}$$

and a quantity

$$l_v \equiv \frac{\eta^2}{\gamma\rho}, \tag{2}$$

which we will call the viscous length. In the Stokes regime, at each instant the flow velocity is such that there is a balance between the viscous forces and surface tension. At first sight, it would appear that the requirement for the Stokes flow is the condition $\mathrm{Su} \ll 1$, or, equivalently, when the viscous length is much larger than the radius of the drop. However, it is necessary to justify this more carefully since in the early stage of coalescence, the radius r_n of the neck between the two drops is much smaller than R_0 and thus one can construct a second dimensionless quantity r_n/R_0.

There have been many attempts to determine the shape evolution by solving the Navier-Stokes equation either analytically or numerically. Among these efforts, Frenkel [3] gave a theoretical analysis based on the assumption of the Stokes flow. He equated the change in the surface energy to the energy dissipated by the viscosity. By making an assumption about the nature of the velocity field in the vicinity of the growing neck, he arrived at the result

$$\frac{r_n}{R_0} = \left(\frac{3\gamma t}{2\pi R_0 \gamma}\right)^{1/2}. \tag{3}$$

Later, Hopper [4] pointed out that the Frenkel's result was flawed due to the incorrect assumption about the form of the flow. In Hopper's study, he gave an analytical solution for coalescence in two dimensions, i.e., for the coalescence of two infinitely long cylinders [5–7]. His calculation showed that when the cylinders are surrounded by an inviscid fluid or by no fluid, immediately after the coalescence starts

$$\frac{r_n}{R_0} \approx \frac{t\gamma}{\pi R_0 \eta}\left|\ln\frac{t\gamma}{R_0 \eta}\right|. \tag{4}$$

This holds when $r_n \ll R_0$.

Eggers *et al.* [8] considered the three-dimensional problem. They pointed out that during the early stage of the coalescence, since the flow at the neck is driven by the highly curved meniscus, the result should be asymptotically the same as in two dimensions, i.e., Eq. (4) should apply. Furthermore, they argued that the local Reynolds number Re near the meniscus should be of the order of $\rho\gamma r_n/\eta^2$. Thus, immediately after coalescence starts, $\mathrm{Re} \ll 1$ will hold regardless of the actual properties of the fluid. The condition $\mathrm{Re} \ll 1$ will continue to hold throughout the time interval in which $r_n \ll l_v$, where l_v is the viscous length scale already introduced. However, l_v is often very small. For water, $l_v = 140$ Å and for mercury $l_v = 4$ Å.

In the later stage of shape evolution when $r_n \gg l_v$, the liquid can be considered inviscid and a simple power law can be derived from the Euler equation which when $r_n \ll R_0$ gives [9]

$$r_n \propto t^{1/2}. \tag{5}$$

Thus, the progress of coalescence of two liquid drops consists of three phases. First, the two interfaces rupture at some point and establish a liquid bridge in between [see Fig. 1]. Second, when $r_n \ll l_v$, the flow is in the Stokes flow regime near the neck and follows the Stokes equation. Third, when

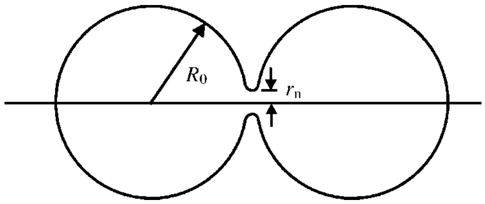

FIG. 1. Sketch of two drops in the early stage of coalescence. The initial radius is R_0 and the radius of the neck is r_n.

$r_n \gg l_v$, the liquid can be considered inviscid and follows the Euler equation.

Recently, Menchaca-Rocha *et al.* [10] reported an experiment carried out with mercury. They studied the coalescence of two mercury drops each of radius 0.05 cm. They were able to measure the neck radius r_n once it had reached 0.015 cm, i.e., a value much larger than l_v, but only one third of the initial radius. By making a fit to the measured r_n with a power-law $r_n \propto t^\alpha$, they obtained α between 0.41 and 0.55, close to the value $\alpha = 1/2$ for coalescence of inviscid liquid drops described by Eq. (5). In this paper we report on measurements in the early stage of coalescence when $r_n \ll l_v$.

II. EXPERIMENT

As already noted, for a fluid such as water, the viscous length scale l_v is so small as to make measurement of the radius of the neck impossible for $r_n \ll l_v$. In addition, the time over which the motion of the fluid is in the Stokes regime is very small. If we assume the neck moves at a speed of γ/η, the time scale t_v for the viscous flow is in the order of $\eta^3/\rho\gamma^2$. For water, this gives a time scale of the order of 10^{-9} s. To make l_v and t_v much larger, we used three samples of DC-200 silicone oil from Dow Corning Inc., with viscosity of $10^3, 10^4$, and 10^5 cS, and density 0.97 g cm^{-3}.

To minimize the effects of gravity, we constructed a Plateau tank as shown in Fig. 2. The tank was initially filled with a mixture of water and *n*-propyl alcohol with a ratio of water to alcohol chosen to achieve a density match with silicone oil. Silicon oil was introduced slowly through openings in the top and bottom of the tank, and the volume of the oil in each drop could be controlled through the two pistons indicated. Around the orifices in the upper and lower surfaces of the cell through which the oil entered was a ridge of radius R_0. The distance from the lower surface of the upper ridge to the upper surface of the lower ridge was $2R_0$. Thus, when sufficient oil was introduced into the cell for the upper and lower drops to make contact, each drop was in the form of a hemisphere.

The surface tension of the interface between the oil and the water-alcohol mixture was measured by the sessile drop method [11]. The result was found to be 9 ± 1 dyn cm^{-1}, the same for each of the oil samples to within the experimental error.

We were able to adjust the density of the alcohol-water mixture by adding water or *n*-propyl alcohol into the tank. The effect of gravity is measured by the Bond number

$$\mathrm{Bo} = \frac{gR_0^2|\Delta\rho|}{\gamma}, \tag{6}$$

where $\Delta\rho$ is the difference between the density of the oil and the alcohol-water mixture. Thus, the effect of a slight density

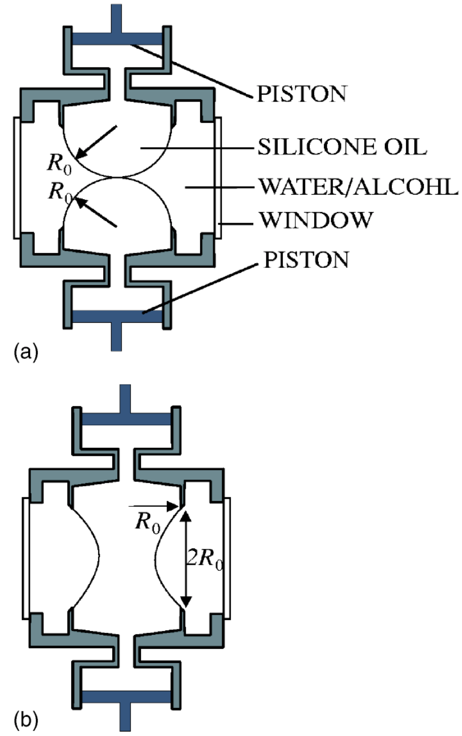

FIG. 2. The Plateau tank for the coalescence experiment. (a) The configuration of the drops just before coalescence occurs. (b) The equilibrium shape of the drops after coalescence.

mismatch increases with drop size. To estimate the density mismatch, we made measurements of the shape of the meniscus after coalescence had occurred and after sufficient time had elapsed so that the interface was no longer moving [see Fig. 2(b)]. The shape of the interface is then governed by the equation

$$\gamma\kappa = \Delta P - gz\Delta\rho, \tag{7}$$

where κ is the sum of the principal curvatures of the surface and ΔP is a constant (see below). Using cylindrical polar coordinates $r-z$,

$$\kappa = \frac{1}{r}\frac{1}{[1+(\partial r/\partial z)^2]^{1/2}} - \frac{\partial^2 r}{\partial z^2}\frac{1}{[1+(\partial r/\partial z)^2]^{3/2}}. \tag{8}$$

The boundary conditions are that $r = R_0$ when $z = \pm R_0$, and the value of ΔP determines the total volume of the oil in the cell. For Bo=0 the pressure difference across the interface of the two fluids is the same everywhere and so the mean curvature is constant. Thus the upper and lower parts of the oil have the same shape. If Bo is nonzero and small, there will still be a stable equilibrium shape, but there will no longer be up-down symmetry. Above a critical value of $|\mathrm{Bo}|$, the bridge will not be stable and will break up [12].

For given assumed values of $\Delta\rho$ and ΔP, it is straightforward to use Eq. (8) to calculate the shape of the interface. These values can then be adjusted to obtain a best fit to the measured shape of the meniscus. This provides a convenient method for the determination of $\Delta\rho$ and Bo. We made measurements for drops with initial radii of 0.5 and 5 cm, and the

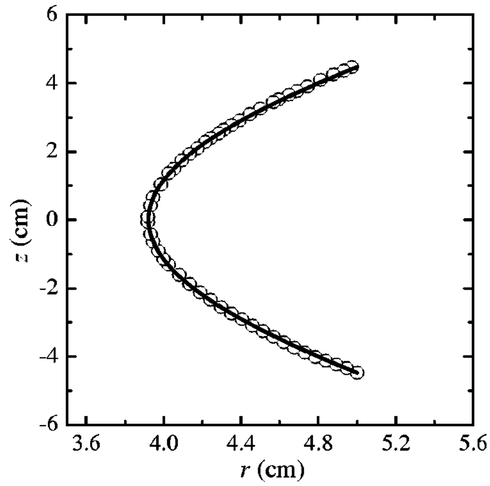

FIG. 3. The equilibrium shape of the liquid bridge after coalescence. The initial radius of the drops was 5 cm. The open circles are the experimental data and the solid line is calculated from Eq. (8) using Bo and ΔP as adjustable parameters.

data for a 5 cm drop are shown in Fig. 3. From the best fit value of $\Delta\rho$, we were able to determine that the density mismatch was 4 ppm, which corresponds to Bo$\sim$0.01. For the smaller drops, the requirement for matching the density is much less critical.

The shape of the meniscus was recorded with a fast-frame camera that can take 1000 frames at 1000 frames per second (256×256 pixels) and a standard home video camera running at 29.97 frames per second (720×480 pixels). Figure 4 shows a series of pictures taken for $R_0=5$ cm. The shape of the meniscus in the last image in this figure is very close to the equilibrium shape.

The neck size as a function of time is shown in Fig. 5. In this figure, we have included data points with r_n as small as $0.1R_0$. For r_n smaller than $0.1R_0$, the measurement of r_n becomes difficult. Ideally, when the two drops approach each other, a bridge between them should form as soon as there is any contact between their two surfaces. This bridge should first appear at a point along the line between the centers of the drops. However, we observed that in our experiment the liquid bridge was not established immediately after the drops came into contact. Consequently, as the two drops continued to approach each other, the surface of both drops deformed slightly and their surfaces were in contact over an appreciable area before coalescence took place. We observed that sometimes two drops could remain with substantial contact without coalescing for a long time, i.e., up to several hours for 5-cm-radius drops. There is a substantial literature on the phenomenon of noncoalescence [13–15]. We have not attempted to investigate how the rupture of the interfaces takes place to establish the initial liquid bridge. The sequence of measurements of r_n as a function of t shown in Fig. 5 was started from the time at which we could first detect a rapid increase in the radius of the neck.

III. ANALYSIS AND DISCUSSION

Based on the measured surface tension, we find that the Suratman number has the values 4.4×10^{-2}, 4.4×10^{-3}, 4.4×10^{-4} for drops of radius 0.5 cm and viscosity $10^3, 10^4$, and 10^5 cS, respectively, and for the 5-cm drop with viscosity 10^5 cS, Su$=4.4\times10^{-5}$. Thus, for all of the drops measured, the flow should be in the Stokes regime, i.e., the inertia of the fluid should not be relevant. It follows that the radius of the neck at time must be given by the scaling formula

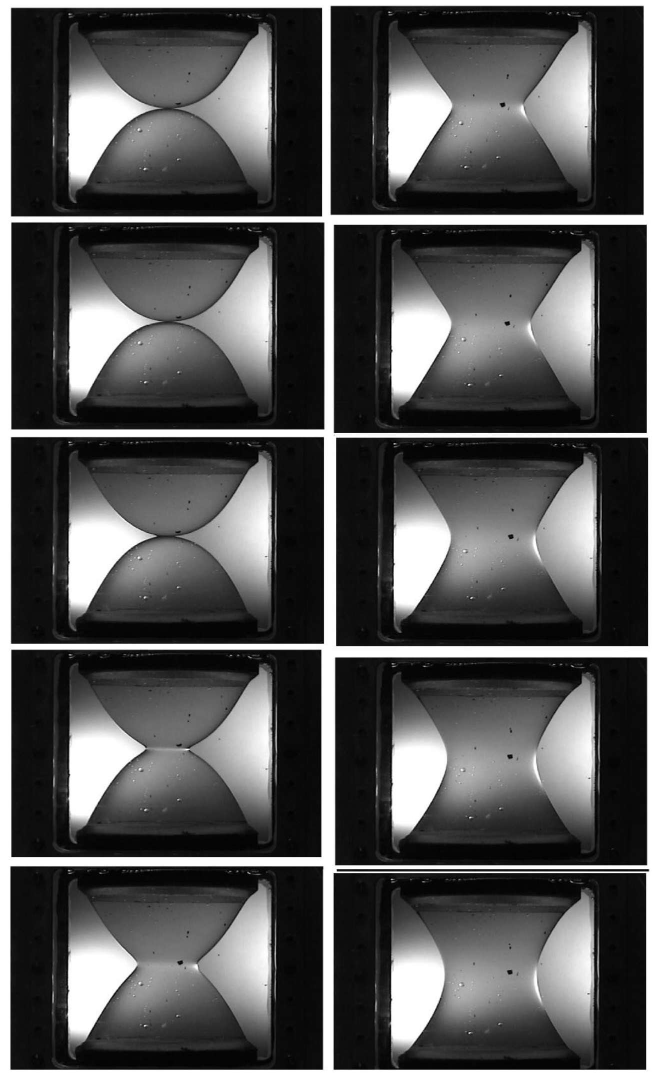

FIG. 4. The coalescence of two hemispheres of initial radius $R_0=5$ cm. The time lapse between the images is 120 s. The shape shown in the final image (bottom right) is very close to the equilibrium shape.

$$\frac{r_n}{R_0} = f\left(\frac{t}{\tau}\right), \tag{9}$$

where

$$\tau = R_0\eta/\gamma, \tag{10}$$

and f is some function. Note that Eqs. (3) and (4) are of this general form. We can use our data to test whether it is consistent with the form of Eq. (9). In Fig. 6, we show a plot of r/R_0 as a function of t/τ for the four drops that we have studied. It can be seen that the scaling formula Eq. (9) is obeyed within experimental error, even though the viscosity

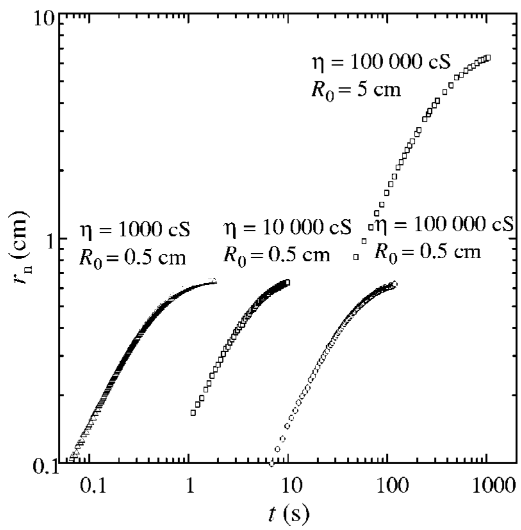

FIG. 5. The radius of the neck as a function of time after the onset of coalescence for drops with viscosity of $10^3, 10^4$, and 10^5 cS, and initial radius R_0=0.5 and 5 cm.

ranges over two orders of magnitude and the radius over one order.

As already mentioned, there is some uncertainty regarding the correct choice of the zero of time. This uncertainty affects the plots of r_n as a function of time. To avoid this problem we can instead consider how the neck velocity v_n varies with the radius r_n, since this relation is unaffected by the choice of the origin of time. In the Stokes regime it should be true that

$$\frac{v_n \eta}{\gamma} = g(r_n/R_0), \tag{11}$$

where g is another function that can be related to the function f. Thus, a plot in terms of the scaled variables $v_n\eta/\gamma$ and

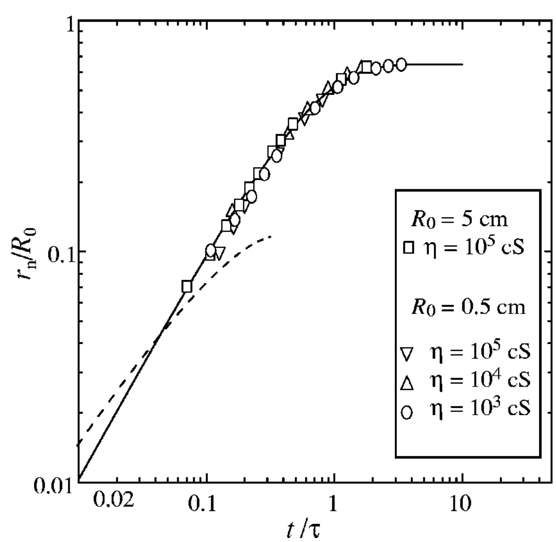

FIG. 6. Plot of the radius of the neck r_n divided by the initial drop radius R_0 as a function of the time t divided by the scaling time τ. The solid curve is a plot based on Eq. (13), and the dashed curve is the result predicted by Eq. (4).

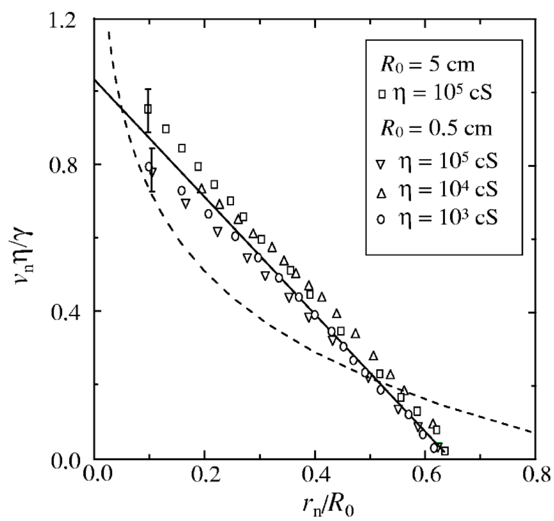

FIG. 7. Plot of the rate of growth v_n of the neck divided by the scaling velocity γ/η as a function of the radius r_n divided by the initial drop radius R_0. The solid line is the fit to the data described in the text, and the dashed curve is the result predicted by Eq. (4).

r_n/R_0 should give the same curve for each drop. It can be seen from Fig. 7 that when plotted in this way, the results from the four different drops are in close agreement. Moreover, the scaled velocity appears to vary linearly with the scaled neck radius. A fit to the data gives

$$\frac{v_n \eta}{\gamma} = a - b\frac{r_n}{R_0}, \tag{12}$$

with $a=1.0\pm0.1$ and $b=1.6\pm0.2$. From Eq. (12), follows the result:

$$r_n = \frac{aR_0}{b}[1 - e^{-b\gamma t/(R_0\eta)}]. \tag{13}$$

A plot of this relation is included in Fig. 6, and it can be seen that Eq. (13) gives a good fit to the experimental data.

Finally, we consider the relation of these results to the theory of Eggers *et al.* [8] and Hopper [see Eq. (4)]. We have included in Figs. 6 and 7 curves that show the predicted variation of r_n with t, and v_n with r_n, based on this theory. It can be seen that the theory is not in agreement with the experimental results. However, as Hopper has emphasized [4], while Eq. (4) appears to be the correct limiting form for small t/τ, it is not a good approximation unless t/τ is *extremely* small. We suspect that this is the reason for the disagreement between experiment and theory. We hope to report measurements for significantly smaller values of t/τ and r_n/R_0 in a subsequent paper.

ACKNOWLEDGMENTS

This research was supported by NASA Grant No. NAG8-1774. One of the authors (W. Y.) would like to thank T. Powers for a helpful discussion.

[1] L. Rayleigh, Proc. R. Soc. London **28**, 406 (1879).
[2] O. Reynolds, Philos. Trans. R. Soc. London **177**, 157 (1886).
[3] J. Frenkel, J. Phys. (USSR) **9**, 385 (1945).
[4] R. Hopper, J. Am. Ceram. Soc. **76**, 2947 (1993).
[5] R. Hopper, J. Fluid Mech. **213**, 349 (1990).
[6] R. Hopper, J. Fluid Mech. **243**, 171 (1992).
[7] R. Hopper, J. Am. Ceram. Soc. **76**, 2953 (1993).
[8] J. Eggers, J. R. Lister, and H. A. Stone, J. Fluid Mech. **401**, 293 (1999).
[9] L. Duchemin, J. Eggers, and D. C. Josserand, J. Fluid Mech. **487**, 167 (2003).
[10] A. Menchaca-Rocha, A. Martínez-Dávalos, R. Núñez, S. Popinet, and S. Zaleski, Phys. Rev. E **63**, 046309(2001).
[11] A. Adamson, *Physical Chemistry of Surfaces*, 5th ed. (Wiley, New York, 1990).
[12] B. J. Lowry and P. H. Steen, Proc. R. Soc. London **A449**, 411 (1995).
[13] M. A. Rother, A. Z. Zinchenko, and R. H. Davis, J. Fluid Mech. **346**, 117 (1997).
[14] G. P. Neitzel and P. Dell'Aversana, Annu. Rev. Fluid Mech. **34**, 267 (2002).
[15] A. Zdravkov, G. Peters, and H. Meijer, J. Colloid Interface Sci. **266**, 195 (2003).